Final Technical Report

Advanced Collision Detection and Site Monitoring for Avian and Bat Species for Offshore Wind Energy

DE-EE0008733

December 7, 2022

Principal Investigators:

- Roberto Albertani, Associate Professor, School of Mechanical, Industrial and Manufacturing Engineering, Oregon State University
- Matthew L. Johnston, Associate Professor, School of Electrical Engineering and Computer Science, Oregon State University

Research Partners:

- Kyle Clocker, School of Electrical Engineering and Computer Science, Oregon State University
- Cassandra Davis, School of Electrical Engineering and Computer Science, Oregon State University
- Nicholas Drachnik, School of Mechanical, Industrial, and Manufacturing Engineering, Oregon State University

Acknowledgment: This material is based upon work supported by the U.S. Department of Energy's Office of Energy Efficiency and Renewable Energy (EERE) under the Wind Energy Technologies Office Award Number DE-EE0008733.

Advanced Collision Detection and Site Monitoring for Avian and Bat Species for Offshore Wind Energy

Final Technical Report

DE-0008733

Table of Contents

1. List of Abbreviations

Abbreviation	**Definition**
3D	Three dimensional
ADC	Analog-to-digital converter
AP	Access point
CAD	Computer-aided design
CMOS	Complementary metal-oxide semiconductor
DOE	Department of Energy
HR	High resolution
IC	Integrated circuit
IMU	Inertial Measurement Unit
IP67	Ingress Protection Rating 67 (IEC 60529)
IR	Infrared wavelengths
LoRaWAN ®	Long Range Wide Area Network
LOS	Line-of-sight
MW	Megawatt (10^6 Watts)
NEPA	National Environmental Policy Act
NIR	Near infrared wavelengths
NREL	National Renewable Energy Laboratory
NWTC	National Wind Technology Center
OSU	Oregon State University
PCB	Printed circuit board
PVDF	Polyvinylidene fluoride
RF	Radio frequency
SNR	Signal-to-noise ratio
SOPO	Statement of Project Objectives
USB	Universal Serial Bus
Vis	Visible light wavelengths

2. Project Overview

Project Summary

The aim of this project was to design, build, and test a persistent and autonomous monitoring system for avian and bat collisions with offshore wind turbines blades and structures. A high-level architecture for the proposed collision detection and image capture system for wind turbine blade strikes is illustrated in **Fig. 1**. The system comprises four primary sensor modules: 1) on-blade sensor modules for collision detection and dual-vision image capture on each blade with both visible light and near-infrared imagers; 2) additional on-blade collision sensors mounted further from the root; 3) a nacelle-mounted unit including a 360º camera and ultrasonic microphone array; and, 4) an on-blade, high-performance infrared camera module. All sensor modules can be controlled over wireless connections. A primary function of the integrated system is the automatic recording of images when a blade strike is detected, with images of the striking object stored for offline analysis of animal type and species.

Primary targeted outcomes were high sensitivity for the detection of blade strikes from bats and small birds, and automatically captured visual confirmation of the striking object; these features are critical for monitoring offshore wind turbine installations, where ground-based methods are not viable. In addition, local recording will provide a long-term sensor recording database. Project tasks comprised: 1) Implementation of core hardware and software components for collision detection, on-blade image capture in visible and infrared wavelengths, and on-nacelle audio/video recording; 2) Standalone and integrated laboratory validation of all components; and, 3) Multiple field studies using both an unattached grounded wind turbine blade and up-turbine at an experimental wind turbine. Following laboratory validation, field testing was be conducted on an operational wind turbine in collaboration with the National Wind Technology Center at the NREL Flatirons campus over two planned field tests.

Project Impact

Wind turbines serve an increasing proportion of total energy generation, with expanded onshore and offshore installations proceeding worldwide. Continued construction, expansion, and operation of wind energy installations must be managed in conjunction with effects on local and migratory wildlife, specifically bird and bat species that may be affected by wind turbine collisions [1]. Ongoing efforts to measure and mitigate wind turbine impacts on wildlife include improved preconstruction siting and postconstruction monitoring, development of wildlife deterrent technologies and real-time curtailment strategies, and improved quantitative assessment of wildlife mortality due to wind turbines [2-4]. Current automated monitoring solutions leverage cameras on the ground or mounted on the wind turbine tower for recognition of nearby birds and can include audible deterrents or automated curtailment of turbine operation. However, these approaches cannot provide physical verification of blade strikes or images of colliding objects, both of which are critical for quantitative assessment of wildlife impacts.

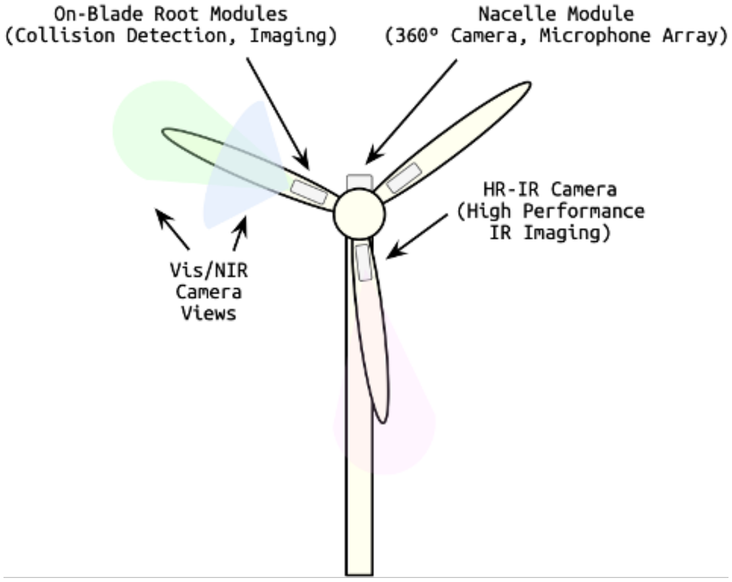

Figure 1. High-level overview of automated collision detection and audio/video capture system for monitoring bird and bat strikes on offshore wind turbines.

Toward the goal of long-term, automated blade strike monitoring, we are developing an intelligent, automated multi-sensor system designed for installation on offshore wind turbines to provide real-time collision detection along with image capture of colliding objects; this may also provide value for wind turbines deployed on land, as well. The sensor system comprises a blade-mounted sensor module that uses accelerometers, gyrometers, and contact microphones to measure vibrations from the blade surface near the hub for collision detection, and cameras focused toward the blade tip that enable video and still image recording sighting along the blade length.

Project Objectives: This project builds on the previous work of researchers at Oregon State University (OSU) funded by the U.S. Department of Energy (DOE) under Funding Opportunity Announcement Numbers DE-FOA-0000414 and DE-FOA-0001554, which included the development and proof-of-concept demonstration of on-blade automated collision detection hardware and on- blade image capture for event confirmation and offline species identification. Field tests were carried out at the NREL National Wind Technology Center (NWTC) in Boulder, CO and at the North American Wind Research and Training Center (NAWRTC) at Mesalands Community College in Tucumcari, New Mexico.

This project greatly extended prior development efforts, as current systems will fail to detect significantly lower energy collision events, including those of bats and small birds. Our approach included investigation of multiple approaches for improving sensitivity: 1) improved sensitivity for collision detection at the blade root; 2) a multi-module sensor system, in which vibration is measured at multiple points along the length of a turbine blade, each using a wireless, low-mass ‘sensor patch’ module; and, 3) developing enhanced impact detection algorithms using machine learning.

In addition, the proposed system augments visual capture capabilities, critical for offshore operations. Nighttime or poor visibility conditions were addressed using a compact, low-cost near infrared (NIR) camera in each root module, as well as investigation of the use of a high-resolution infrared (IR) camera on blade as a reference. As image recording for blade strike confirmation using a single camera may be problematic for longer blades, the system includes two on-blade cameras for dual-focused (near and far) vision to extend visual coverage range along the length of the blade. Finally, to support offshore monitoring of birds and bats, a wide-bandwidth microphone was integrated into a nacelle-mounted module for audio recording at the moments of a blade or other structure strikes.

Project Outcomes: The integrated sensor system is intended to address critical needs for validation and siting or wildlife impact minimization technologies without human operators. Project outcomes include a validated approach and system architecture for automated blade collision detection, analysis of both low-cost and high-performance on-blade imagers of daytime and nighttime image capture, and a suite of trained collision detection algorithms that will continue to improve with additional data from field testing or future deployments. In addition, future commercial systems guided by this development can provide a local, long-term sensor recording database for each deployment site, as well as time stamping and recorded wind turbine conditions at the time of any detected impacts.

Future version of this system can fill an existing void in wind energy environmental impact minimization, mitigating a current market barrier. Such systems can monitor and mitigate negative impacts to wildlife from increasing wind energy infrastructure, as well as providing new mechanisms for understanding the impacts of wind turbines to avian and bat species offshore more broadly.

3. Summary of Technical Objectives and System Components

Tasks, subtasks, and milestones in the negotiated Statement of Project Objectives (SOPO) were organized roughly by system component, including design, implementation, and validation of each primary component (on-blade root sensor/imager module, on-blade sensor patch, on-blade high-performance IR imager module, on-nacelle video/audio module) and of integrated system-level testing of multiple components. In this section, we summarize progress to date in each of these areas and toward all subtasks in Task 1.00, Task 2.00, and Task 3.00.

3.1. Collision Detection System – Blade Root Modules, Cameras, and Sensor Patches (Task 1.00)

Design, implementation, and test of on-blade root module

A high-level architecture of the on-blade root module was initially completed, including block-level specification of sensors interfaces such as number and type of accelerometers, gyrometers, and contact microphones; functional requirements of on-board computation, wired/wireless interfaces; and, dual-camera support. Primary components and block-level architecture are illustrated in **Fig. 2**, which include custom electronic printed circuit board (PCB), two single-board computers for video capture and wireless data interfacing, support for up to four external contact microphones, and two side-by-side camera modules (similar to cell phone cameras).

The core sensor electronics are housed on a custom-design PCB, which includes:

- An integrated inertial measurement unit (IMU) that includes 3-axis accelerometer and 3-axis gyrometer, both with 16-bit resolution (Bosch BMI088) with up to 2kHz data output rate.
- Custom analog front-end amplifier circuits and analog-to-digital converters (ADC) supporting up to four separate contact microphones, as needed. For the current design, two of these contact microphone interfaces are used for external sensors at the root module.
- High-performance microcontroller for real-time data processing of IMU and contact microphone data (XMOS XUF216), more typically used in commercial audio applications for real-time multichannel audio signal processing.
- On-board power management for all components.

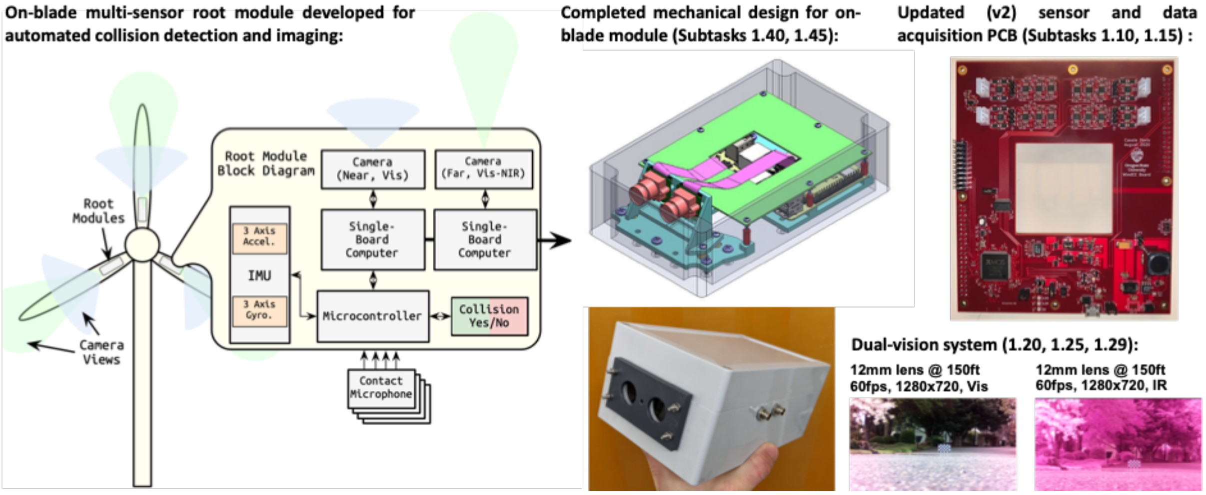
On-blade multi-sensor root module developed for automated collision detection and imaging:

Completed mechanical design for on-blade module (Subtasks 1.40, 1.45):

Updated (v2) sensor and data acquisition PCB (Subtasks 1.10, 1.15) :

Dual-vision system (1.20, 1.25, 1.29):

Figure 2. (left) Block diagram of multi-sensor on-blade root module, which includes accelerometers, gyrometers, and contact microphones for collision detection and dual low-cost cameras for near/far down-blade imaging. (right) Design and implementation of the assembled and tested root sensor module, as well as representative test images from imager characterization.

The PCB was designed at Oregon State University using industry-standard CAD tools and fabricated using an external vendor. A preliminary prototype version (not shown) was used for hands-on investigation of multiple accelerometer/gyrometer parts and for initial development of microcontroller and contact microphone interfaces to assess performance and interconnection. A second and final root module sensor PCB was designed and fabricated (shown in **Fig. 3**), which was used for all subsequent testing.

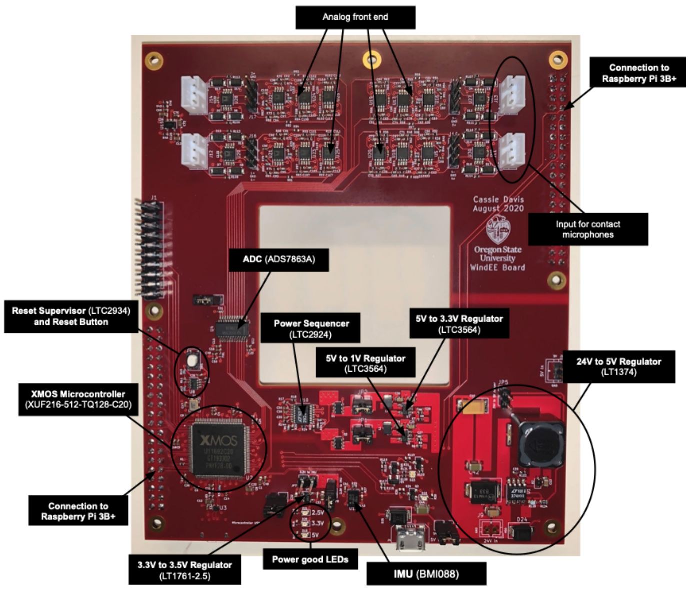

Figure 3. Annotated photograph of custom multi-sensor electronic printed circuit board (PCB) developed as the core of the on-blade root sensor module.

Evaluation of on-blade camera modules:

As shown in **Fig. 2**, the root module includes two cameras to provide visible light and near-infrared imaging capabilities, as well as to support dual-vision (near/far) cameras for enhanced imaging sighted along the blade length. The selected camera modules (Raspberry Pi v2, normal and NoIR versions) include 8MP CMOS image sensors and support multiple operational modes, including 1280x720 (720p) at 60 frames per second (fps).

Prior to integration in the root module, imagers and interfaces were acquired and successfully set up for evaluation of pixel density, frame rate, and synchronization. Systematic assessments of image, distance,

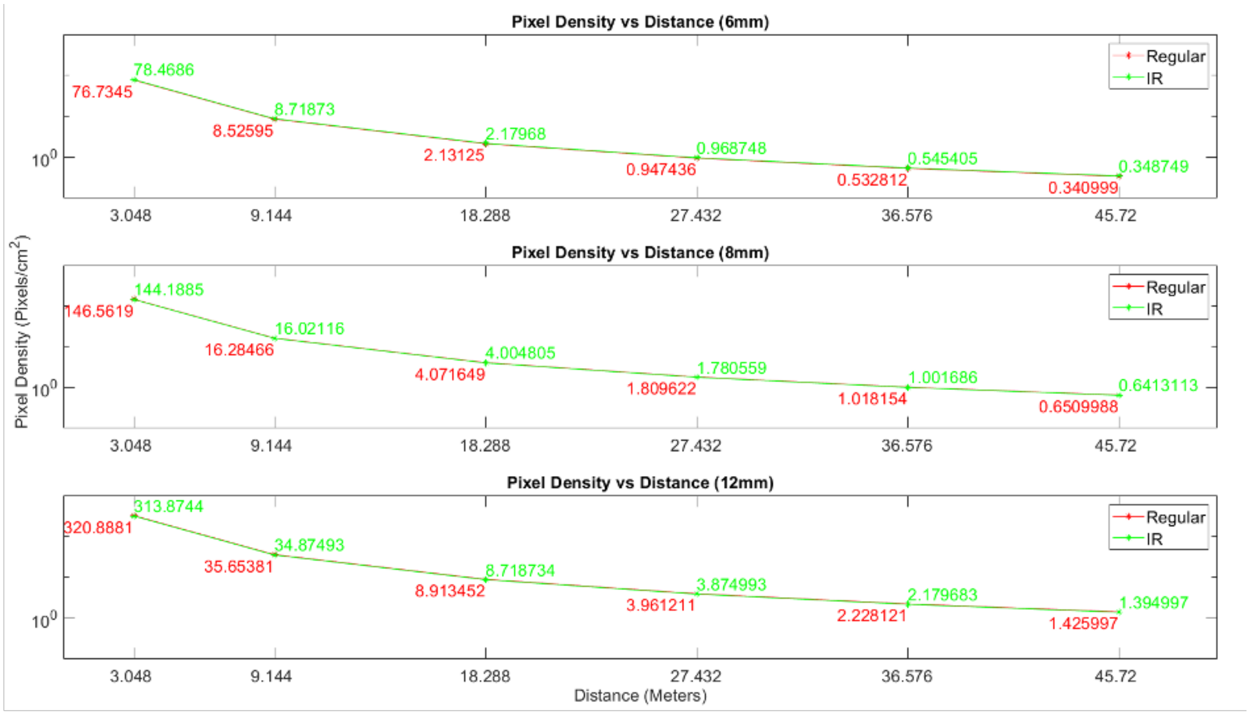

Figure 4. Pixel density as a function of distance for regular and IR camera modules, calculated from recorded test images; example images with standard test grid are shown in Fig 2. Both camera modules use the same 8MP pixel sensor, so pixel density is the same for both modules and in both bright light and low light.

and resolution were completed using a standardized test grid for both the daylight and near-infrared camera modules. Following testing, data analysis was completed to assess imager performance and pixel density for both camera modules; pixel density is the same for both daylight and NIR imagers, as both modules use the same 8MP image sensor, and is summarized in **Fig. 4.**

Software and firmware development:

Custom firmware was developed that runs on the core sensor PCB microcontroller in the root module; this code is responsible for managing data readout and data processing from sensor interfaces (IMU and contact microphones). Initial firmware development was completed using a commercial evaluation board for the core microcontroller used in the root module design, including firmware interfaces for all selected accelerometer/gyrometer ICs.

Custom software was developed for the root module single-board computers, which includes data import from the sensor PCB board for recording and wireless data access, control and recording of the two on-blade cameras, and automated video capture following collision detection.

Root module hardware design and assembly:

The root module mechanical envelope was selected, using as a base (i.e. prior to custom modification) the same weather-proof enclosure previously used and validated for size and mass in prior up-turbine testing at NREL-NWTC [17]. Placement of primary components (sensor board, root module computers, dual-vision cameras) was planned to using a custom 3D CAD model of the root module system. Following completion of the mechanical design and fixturing of the root module, component manufacturing, including all custom machined and 3D printed components, and custom housing modifications, were completed. Both CAD model and fully-assembled root sensor module are shown in **Fig. 2**.

High-resolution infrared (HR-IR) camera investigation:

In addition to the Vis-NIR camera module including in the root module, the system includes a separate, standalone high-performance IR camera module for on-blade use. A primary goal is the evaluation of such an imager for night-time, on-blade imaging, and a direct comparison of the relative performance of a high-cost, high-performance (longer IR wavelength) IR camera vs. the low-cost, lower-performance camera module for use in enhancing night-time visibility along the wind turbine blade.

A variety of HR-IR camera options from multiple vendors were assessed for cost, performance, and interface tradeoffs. A camera module was selected (Sierra Olympic Viden 75LR) and acquired; this model provides remotely operated zoom / focal length adjustment to maximize experimental data that can be acquired during limited on-blade testing.The model requires a custom housing for on-blade use, which was designed using a CAD model; both camera and housing design are shown in **Fig. 5.** The housing was fabricated by modifying a commercial ingress protection (IP) rated IP67 enclosure, similar in size to the root module enclosure.

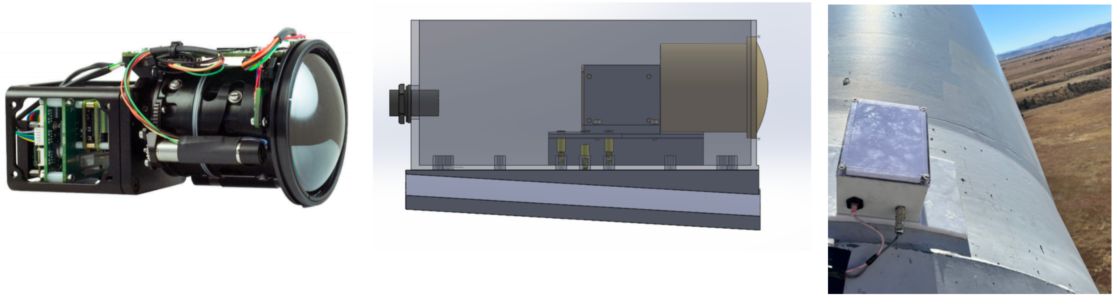

Figure 5. (left) High-performance IR camera selected for use in on-blade IR imaging investigation (Sierra Olympic Vinden 75LR). (middle) CAD model of custom enclosure for on-blade mounting of IR camera using a modified IP67 polycarbonate enclosure. (right) Installed IR camera on a wind turbine blade near the root, with field of view facing toward the blade tip; images shown in Section 3.

Multi-module sensor patch development:

As illustrated in **Fig. 6**, the distribution of vibration/collision detectors along the length of the turbine blade can increase detection sensitivity and possibly provide localization of the blade strike. Toward this end, we developed several generations of wireless vibration sensor 'patches' for multi-point impact detection along the blade length. Specific technical challenges to investigate include low-power vibration sensing, energy harvesting, and wireless communication modes (e.g. RF and acoustic) for multi-sensor data communication.

Architectural investigation for sensor patches included evaluation of energy harvesting approaches (e.g. piezoelectric, kinetic, solar) and low-power collision detection approaches. Solar energy harvesting was selected due to the availability of thin (<1mm), flexible, low-mass photovoltaic cells and their relatively high-power output. A monocrystalline silicon solar cell was chosen for its low-cost high efficiency, and suitability for long term outdoor use. A commercial energy harvesting microchip (ADP5091) is used to manage the energy harvesting to power the patch. It operates at low (sub-µW) power and is able to charge a coin cell battery from a solar cell. This approach is suitable for the patch which must operate indefinitely without battery replacement, but which need not perform high-power operation, such as wireless transmission, continuously. As such, the patch can continually 'listen' for a collision at lower power (µW), and then 'wake up' for detected collisions to send a wireless alarm to the root module (mA).

Behavioral simulations were developed for the sensor patch operation, including investigation of needed sample rate and resolution, as well as the investigation of low-power collision detection approaches with integrated classification. Multiple low-power contact sensors have been experimentally characterized for use as impact/vibration transducers in the sensor patch, including ceramic piezoelectric sensors and thin-film polymer (PVDF) piezoelectric sensors; the latter have been selected for low mass, mechanical flexibility, and high sensitivity.

The first version of the sensor patch included a multi-band microcontroller for wireless communication using Zigbee, which is similar to WiFi and common in IoT devices. Later versions of the sensor patch modules for up-turbine testing used Bluetooth (range of tens of meters) and finally LoRaWAN (range of 1 km or greater), the latter of which provide the longest sensor range for wireless communication from the nacelle, ground, or nearby field station.

The patch architecture was designed and implemented using a custom electronic printed circuit board, including solar energy harvesting, two contact microphone front-end amplifiers, and ultra-low-power on-board computation (**Fig. 6**). Patch sensor modules were validated prior to laboratory and field-based testing. The system is housed in a modified ingress protection (IP) rated IP67 enclosure and affixed to the wind turbined blade using an aluminum mounting plate (additional details in Section 4).

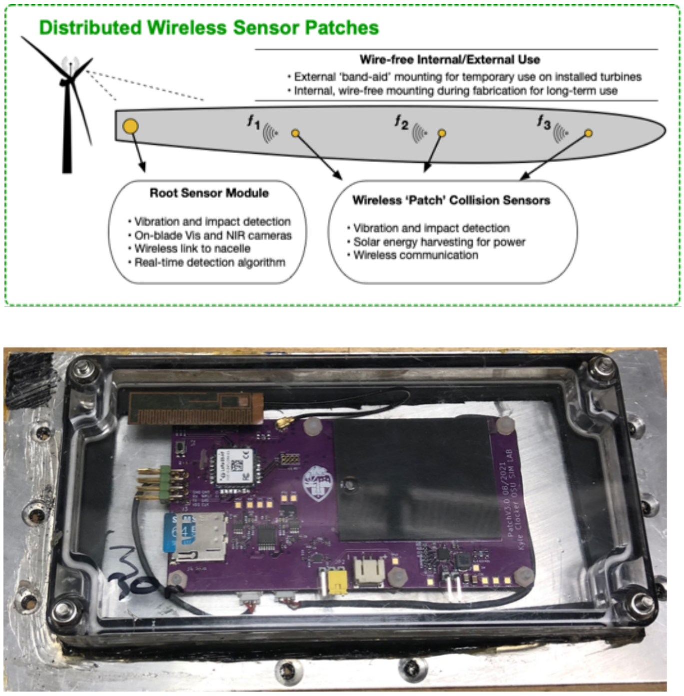

Figure 6. (top) Distributed sensor 'patches' on the blade provide localized collision detection to improve system sensitivity. (bottom) The core of the sensor patch is a custom electronics module providing solar energy harvesting and wireless data.

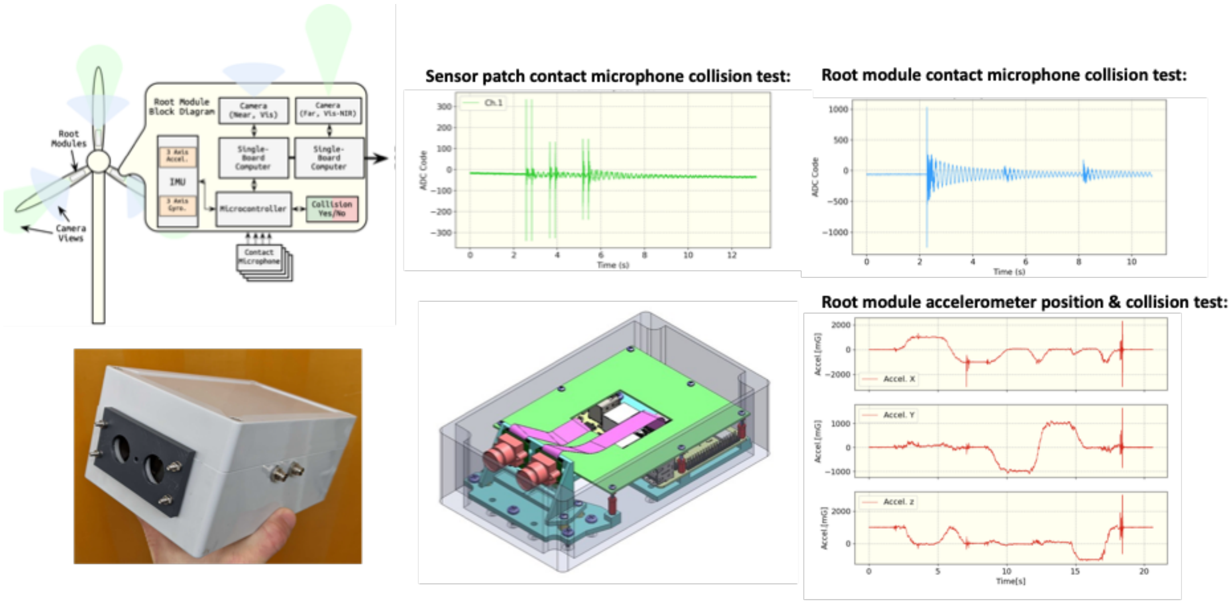

Figure 7. Typical results from laboratory testing of all root module and sensor patch components as an integrated system, including root module accelerometer and contact microphone, root module dual-vision imagers, sensor patch contact microphones, and wireless control and data interfaces. All systems were successfully validated; additional details are provided in the Deliverable 1.79 report attached to this continuation application.

Complete system integration and lab tests:

Following standalone verification and system-level integration of all root module sensors, imagers, and sensor patch devices, the complete collision detection and automated imaging system was tested in a laboratory setting, primarily in preparation for on-site field testing on a full-size, unattached wind turbine blade. For these tests, a test fixture was constructed as a lab-scale (~2m) suspended beam, with root module attached at the anchored beam end, and sensor patches tested on the beam surface. A few representative figures are shown in **Fig. 7**.

The primary purpose of the lab tests was to verify primary functionality of all collision detection and automated image capture components. This includes: main root module accelerometer, gyrometer, and contact microphone sensors for collision detection; on-blade sensor patches with contact microphones and wireless link for distributed on-blade collision detection; on-blade camera modules (normal and near-IR) with automated video recording following collision detection; and, all software and firmware required for wired and wireless communication and data transfer among all system components.

All primary system functions were successfully validated, including root and patch sensors, as well as automated image capture from the integrated dual-vision camera modules following a detected collision.

In addition to functional verification of all collision detection and on-blade imaging system components, structured laboratory testing was also a critical process for preparing for field testing, illuminating remaining software or firmware errors, interconnection methods, and best practices for structured data acquisition

3.2. Audio/Visual Recording System – Nacelle Module (Task 2.00)

As described in **Fig. 1**, the integrated sensor system includes a nacelle-mounted video and audio recording module to support offshore monitoring of birds and bats. As proposed, this custom system includes a 360º camera and a wide-bandwidth microphone array (including ultrasonic) for recording both bird and bats sounds, addressing the current lack of audio recording at the moments of a blade or other structure strikes.

The nacelle unit architecture was designed using commercial off-the-shelf sensors, including camera and microphones, integrated into a complete system, and fixtured using a custom-modified weather-proof enclosure. The system includes four ultrasonic USB microphones (Ultramic 250K) for 360º coverage. The microphones sample at 250 kS/s and record from human audio range up to a frequency of 96-192 KHz. The enclosure is a modified, weatherproof enclosure with an IP-67 rating. On top of the enclosure is a 360º camera module (Insta360 One R) that is connected wirelessly to a remote control.

Following a design using 3D CAD models, and initial prototype fixture was fabricated and is shown in **Fig. 8.** The enclosure also houses a wireless, single-board computer, which provides data, control, and communication interfaces among the components, including audio recording.

Figure 8. Design and implementation of nacelle-mounted AV unit, including 360º camera module and wideband microphone array for both video and audio capture of nearby birds and bats.

3.3. Preliminary Field Test – Grounded Blade Testing (Task 2.50)

Following system-level integration and laboratory testing of all root module sensors, imagers, and sensor patch devices, the complete collision detection and automated imaging system was tested on a full-size, unattached wind turbine blade in December 2020. These tests were conducted on a 2.1MW turbine blade (~45m in length) stored on the ground at the Avangrid Renewables storage facility near Arlington, OR.

Test siting and selection were conducted in coordination with Avangrid Renewables, and on-site testing was conducted following both NEPA EQ-1 submission and approval as well as approval of all field test and travel plans by Oregon State University through a separate COVID-19 research resumption plan to adhere to all university research and travel restrictions currently in place. The tests were conducted across five on-site days, included installation and verification, extensive testing to assess collision detection sensitivity and on-blade imager resolution, and removal of all equipment and test articles from the site.

The primary purpose of the field tests was to verify primary functionality of all collision detection and automated image capture components on a full-size wind turbine blade, and to assess collision detection accuracy for multiple low-energy impact levels. Tested integrated system components include: main root module accelerometer, gyrometer, and contact microphone sensors for collision detection; on-blade sensor patches with contact microphones and wireless link for distributed on-blade collision detection; on-blade camera modules (normal and near-IR) with automated video recording following collision detection. Representative figures are shown in **Figs. 9-11**.


Unattached wind turbine blade marked off for testing: **Root module and contact microphone installation:** **Sensor patch test installation:**

Figure 9. Initial field testing conducted on an unattached wind turbine blade stored on the ground, including installation and validation of all on-blade collision detection and imaging components, following by extensive collision testing using surrogate projectiles and a force-measurement impact hammer. On-blade imager testing, automated image capture of blade strike object, and patch wireless communication range were also validated.

Two parametric collision and impact energy experiments were performed: 1) an impact hammer with force readout was used for measured impact force experiments at three energy levels, culminating in >250 impacts recorded simultaneously across all system sensors; and 2), a table tennis ball launcher was used for repeated collisions using a 2.5g projectile at three impact velocities, resulting >140 impacts recorded simultaneously across all system sensors.

Functional verification of all primary system components on a full-scale wind turbine blade was successful, including testing of the integrated collision detection and automated on-blade image capture systems, leveraging sensor modules at the blade root and along the blade length. All system components communicate wirelessly using WiFi or (for the distributed on-blade sensor patches) Bluetooth networks.

Collision detection accuracy >80% has been demonstrated through two separate experimental approaches during field testing on the integrated system installed on an unattached wind turbine blade on the ground. In both experiments, surrogate collisions were focused near the leading edge of the wind turbine blade to better emulate real-world blade strikes.

For estimating the impact energy of a soft projectile, a quantified impact/impulse hammer with soft tip was used to impart blade strike energy in a measurable and controlled manner, as shown in Fig. 10. From these test results, a force on 27 N was recorded with 100% system-level detection rate. According to the volant impact model used to correlate bird collisions with force [5], such force applied to a 10 g mass could correspond to a 0.100 m length body, typical for a silver-haired bat, for example, at an impact velocity of 16.4 m/s.

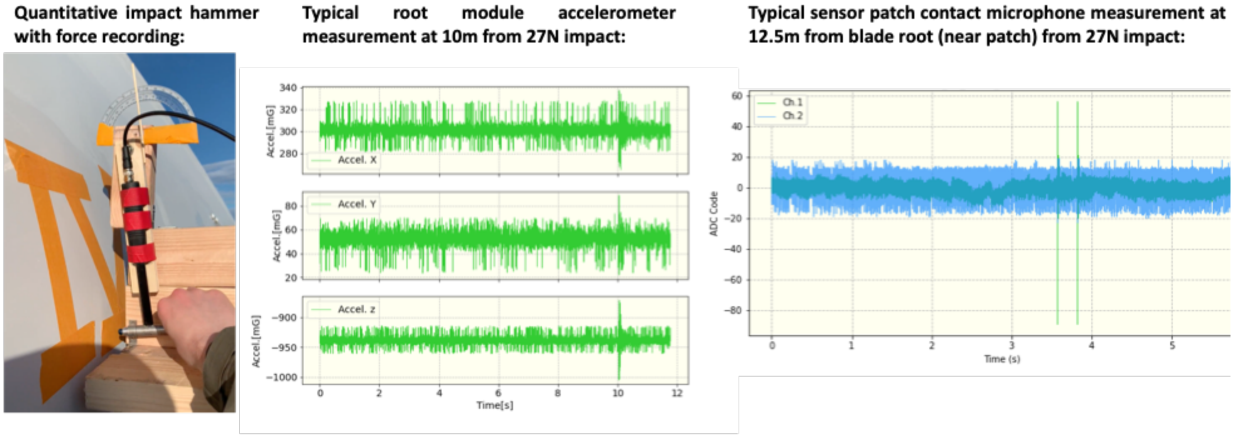
Quantitative impact hammer with force recording: **Typical root module accelerometer measurement at 10m from 27N impact:** **Typical sensor patch contact microphone measurement at 12.5m from blade root (near patch) from 27N impact:**

Figure 10. In one set of experiments, a quantitative impact hammer was used to impart measurable impact force for energy calculations. Three impact forces (15º, 30º, 45º starting position) were used across each of 17 marked 2.5m blade sections, with five replicates of each. Typical measured data is shown for root module and sensor patch.

2.5g projectile tests using table tennis ball launcher:

Typical root module accelerometer measurement for 2.5g projectile impact at 10m from blade root, 10 /s velocity:

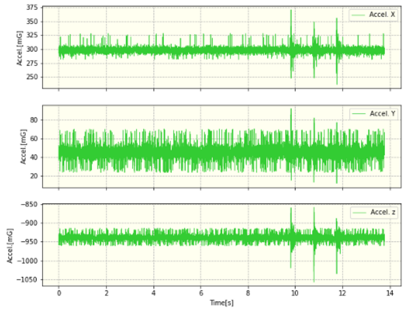

Typical sensor patch contact microphone measurement at 10m from blade root (near patch) for the same impact:

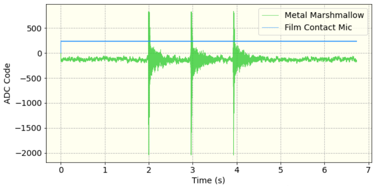

Compiled projectile measurements from root contact microphone 10-30m from blade root with 100% detection:

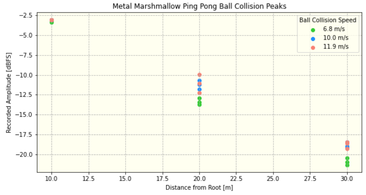

Figure 11. In a second set of experiments, a table tennis ball launcher was used to provide repeatable, low-mass (2.5g) collisions at variable impact velocities. Three impact velocities (7-10 m/s) were used across each of 17 marked 2.5m blade sections, with three replicates of each. Typical measured data is shown for root module and sensor patch.

As shown in Fig. 11, a table tennis ball launcher was used to provide repeatable, low-mass (2.5g) collisions at variable impact velocities. Three impact velocities (7-10 m/s) were used across each of 17 marked 2.5m blade sections, with three replicates of each. Using repeated, velocity-controlled collisions of a table tennis ball surrogate blade strike projectile, we demonstrate 100% detection accuracy for a 2.5 g object striking the blade at 10 m/s (the minimum estimated blade strike velocity – this would typically be much higher). This is validated at up to 30 m from the root module, and patch sensors also demonstrate 100% detection accuracy in these experiments.

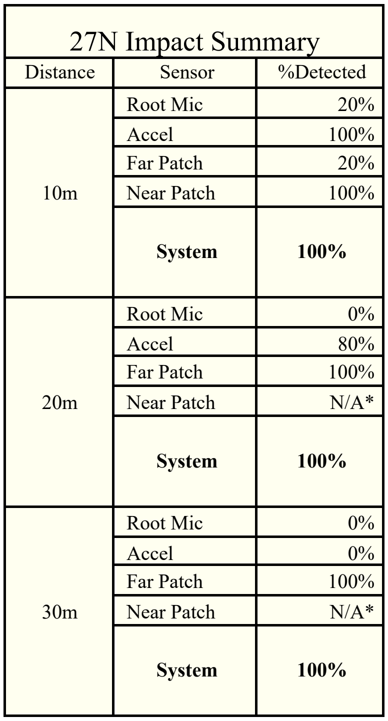

27N Impact Summary

Distance	Sensor	%Detected
10m	Root Mic	20%
	Accel	100%
	Far Patch	20%
	Near Patch	100%
	System	**100%**
20m	Root Mic	0%
	Accel	80%
	Far Patch	100%
	Near Patch	N/A*
	System	**100%**
30m	Root Mic	0%
	Accel	0%
	Far Patch	100%
	Near Patch	N/A*
	System	**100%**

Figure 12. System-level collision detection performance for 27N impact force from impact hammer testing. While the root module sensors alone are unable to detect collisions at 30 m from the root, the inclusion of patch sensors in the system provides 100% collision detection across the tested blade length.

While detection accuracy from experimental impacts is described above, minimum impact energy can be estimated by extrapolating measured data from our full-scale grounded wind turbine blade tests. Impact tests performed on a grounded turbine blade showed a minimum 3σ impact force detectible by the system of 10.0N on the measured SNR contact microphone baseline at 10m; as both root module and sensor patch use the same contact microphone transducer, this is representative of distance from blade root or of distance from nearest patch sensor.

Such force at 3σ from SNR determines the minimum impact energy required to achieve >90% impact detection accuracy and corresponds to the following estimates of collision events using the volant model [5]:

- 10g mass, 100mm length (typical of silver-haired bat) at 10.0 m/s
- 20g mass, 150mm length (typical of hoary bat) at 8.7 m/s
- 300g mass, 250mm length (typical of marbled murrelet) at 2.9 m/s

This approach, while preliminary, demonstrates highly relevant estimated minimum impact energy for use in blade strike detection of bats and small birds. As for the previous GNG criteria, this is achieved using a highly-conservative signal amplitude-based detection method and in anticipated to improve with more advanced algorithms, and it must further be tested in the presence of real wind turbine operational conditions for assessment of long-term real-world utility. However, it remains a promising result from initial field tests.

We note that a) this detection accuracy is demonstrated using a rudimentary and highly conservative detection algorithm and is only expected to improve using our previously developed machine learning classifier approaches once trained on full-scale turbine data, b) this is not done in the presence of operational turbine noise, such as pitching and generating, and thus up-turbine testing is required to assess under real-world conditions, and c) this demonstrates the value and possible requirement for distributed patch sensors for improving sensitivity and detection accuracy at the system level.

An important lesson learned from ground-based testing on an unattached wind turbine blade is the critical need for extensive sensor recordings and system testing before installation on an operational wind turbine. While a useful proxy, a ground-based turbine blade does not provide the background structural-borne noise during turbine operations such as vibrations from gearbox or generator, which cannot be appropriately recreated on a ground blade. Attempts during the field test to introduce useful mechanical noise to the ground-based blade using an automated shaker or tapping devices were not successful and would likely not be representative if achieved. Additionally, due to its placement on multiple blocks for support, the grounded blade responds much differently in terms of vibration and sound propagation compared to a cantilever, root-mounted blade installed on a turbine. As such, the up-turbine field tests are critically required for both assessing and improving system performance in a realistic setting.

3.4. Bridge Task (BP1 to BP2) (Task 3.00)

In preparation for field test planning (Task 4.00), a bridge task comprised the detailed planning required for on-site testing of the complete collision detection and vision system while installed on an operational wind turbine. As outlined in the SOPO, this included two field tests at the NREL Flatirons Campus, which houses the National Wind Technology Center (NWTC).

Regularly recurring test planning meetings with NWTC engineers and coordinating staff began in December 2020 and continue approximately bi-weekly during the bridge task via remote video meetings. A detailed test plan for NWTC was developed in collaboration to address scheduling, logistics regarding hardware installation and validation on the wind turbine, power/data/network interface definitions, as well as both general safety planning and COVID-19 specific safety protocol development.

Final testing occurred over two on-site field tests in June 2021 and October 2021, as detailed in Section 3.

4. Summary of Field Testing on an Operational Wind Turbine (Task 4.00)

Two separate field tests were conducted to validate functionality of the complete integrated detection and imaging system on an operational wind turbine, and to provide real-world data on which to continue to develop, train, and test automated impact detection algorithms. This section summarizes each of these field tests, including installation, data collection, and lessons learned for future development.

4.1. Field Testing at NREL-NWTC, Boulder, CO – June 2021

Field Test Overview

Following system-level integration and field testing of all root module sensors, imagers, and sensor patch devices, the complete collision detection and automated imaging system was tested on an operational 1.5MW GE wind turbine at NREL-NWTC. The first up-turbine test of the complete collision detection system on an operational wind turbine was completed at the NREL Flatirons Campus over a period of eight working days, June 17-28, 2021. Installation of root modules, nacelle module, and all networking hardware was completed in conjunction with NREL staff using planned installation procedures and validated post-installation. The high-performance IR camera module was installed on a blade root, near one of the root module sensor enclosures. An overview of the installed modules is shown in **Fig. 13**.

Installation of blade sensor patches was completed by a rope-based turbine maintenance vendor coordinated directly by NREL, using installation procedures developed and tested during the Bridge Task (Task 3.0). Installation of three wireless sensor patches distributed along the blade at 10m, 20m, and 30m from the blade root was successfully completed, and all modules were verified as functional following installation. A total of three sensor patches was chosen as a balance of coverage (every 10m) and installation time/cost for the testing; while more sensors would provide additional data, this was a feasible number to install, and based on grounded blade testing, should yield sufficient coverage for sensitive collision detection. The chordwise position was selected to assure the lowest possible aerodynamic disturbance but preserving structural relevance. For least intrusion of air flow boundary layer, the location of the patches was on the pressure side of the blade at a chordwise station, approximately 20% of chord from the trailing edge of the blade. The blade structure at that location does not have relevant members except the outside shape.

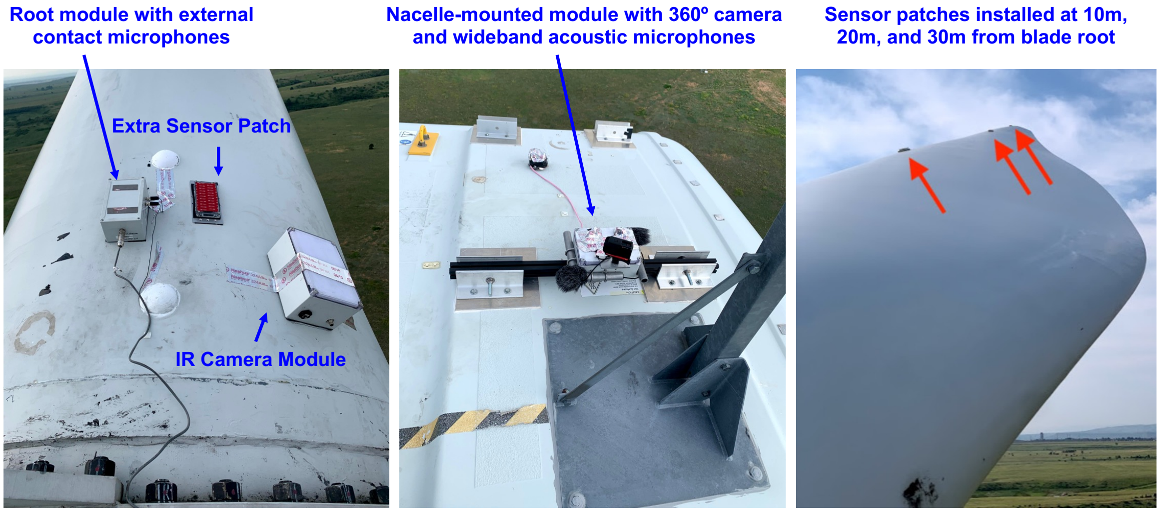

Figure 13. (left) Root module sensor, IR camera module, and extra sensor patch (for testing) installed near the root of a blade on a 1.5MW GE wind turbine; root modules installed on all 3 blades. (middle) A/V recording module installed on the top of the nacelle. (right) Distributed wireless sensor patches installed along the blade length.

Figure 14. Custom gelatin and balsa wood projectiles designed and built on-site at NREL-NWTC were launched at the blade for surrogate

Blade attachment for each sensor patch included an aluminum baseplate bonded to the blade surface with adhesive, and a matching sensor patch plate attached to the baseplate using screws; this approach enables easy installation and removal of the sensor patches for post-experiment analysis, and no drilling into the blade surface itself is required. However, as the vibrations resulting from a collision must travel through both plates to reach a contact microphone, this will somewhat degrade sensitivity compared to direct adhesion of contact microphones to the blade surface. As such, results from a permanently installed system could be expected to be at least as sensitive, and likely more so, compared to measured results.

Multiple tests, including tap testing and extensive surrogate projectile testing using custom gelatin-based projectiles, were completed in alignment with the developed test plan. Data was recorded from root modules and sensor patch modules, as well as audio/video recordings from the nacelle module and IR camera.

For primary collision detection testing, surrogate projectiles were used. Standard tennis balls (~57g) as well as custom balsa and gelatin projectiles (20g and 40g) manufactured on-site at NREL-NWTC (examples shown in **Fig. 14**) were fired toward the turbine blade from a compressed air launcher. Gelatin and balsa are more similar to bird/bat structures, are biodegradable (important for NREL field testing), and with the designed shape are easily targeted for blade strikes. Mass selection was a function of 20g and 40g is within range of small bird and bat species and is also in the range of projectiles masses that can be reliably launched – lower mass projectiles do not track as well, decreasing collision hit rate, and much larger projectiles would necessitate changing to a larger barrel diameter between lighter and heavier projectiles, in turn decreasing test throughput to exchange, test, and re-aim.

Approximately 110 projectiles were launched during testing days, weather and wind allowing, with >80% of these striking the blade. Testing was not possible in the presence of lightning or nearby thunderstorms, for example. For these tests, the blades were not spinning, and the blade with the sensor patches and IR camera was in the downward position to maximize strike likelihood. (Experiments on moving wind turbine blades were completed in a future field test, summarized in Section 3.2).

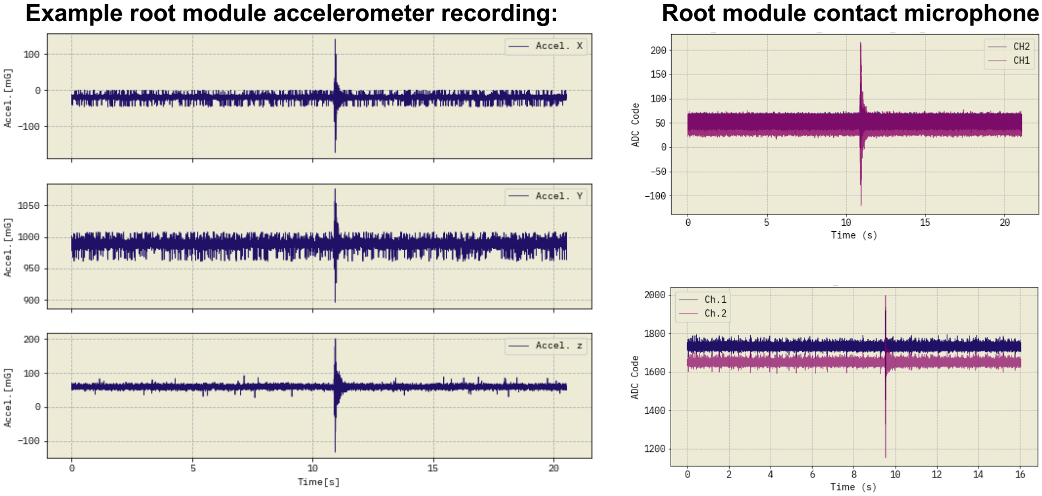

Example root module accelerometer recording:

Root module contact microphone:

Figure 15. Example sensor recordings from the root module sensor platform, including 3-axis accelerometer and 2-channel contact microphones during a blade strike from a surrogate projectile.

Typical sensor recordings from projectile experiments are shown in **Fig. 15** for a blade strike. While data was retrieved from all root module and patch recordings and preliminary analysis complete, detailed analysis was postponed so that efforts could be focused on implementing hardware, firmware, and software changes to address lessons learned in the first field test in advance of the second (final) field test. Primary among these notes and improvements are:

- WiFi connection from an access point (AP) inside the hub to the blade-mounted root modules did not properly propagate through the hub wall. This was updated to use a ground-based or line-of-sight (LOS) WiFi connection for the second testing revision.
- A known error in the energy harvesting chip used inside the patch electronics caused a reset error in the patches when in full/direct sunlight. This was mitigated by partially covering the integrated solar cell but was resolved by a hardware revision of the patch prior to the next round of up-turbine testing.
- LOS was extremely important for maintaining Bluetooth range for sensor patch communication; as installed, the 30m (from root) patch was too far out of range for reliable connection from the root module with the blade in a vertical position. This was addressed by a change to LoRaWAN long-range wireless networking infrastructure in a revised patch implemented in between field tests, which should increase wireless range to 1km or greater.
- For the IR camera, the enclosure was slightly too wide given the install location and blade curvature, which made for difficult installation. This was resolved by adding a custom, curved mounting plate to the bottom of the camera enclosure.
- When installed, the camera was prone to overheating and thermal shutdown in direct sunlight, which caused difficulty in recording video. This was resolved as a camera hardware issue that was fixed in advance of the second field test, yielding significantly more IR camera recording (Section 3.2).
- Installation of the blade patch sensor mounting plates took longer than anticipated. However, as the base mounting plates remained installed for the second field test, patch installation was faster.

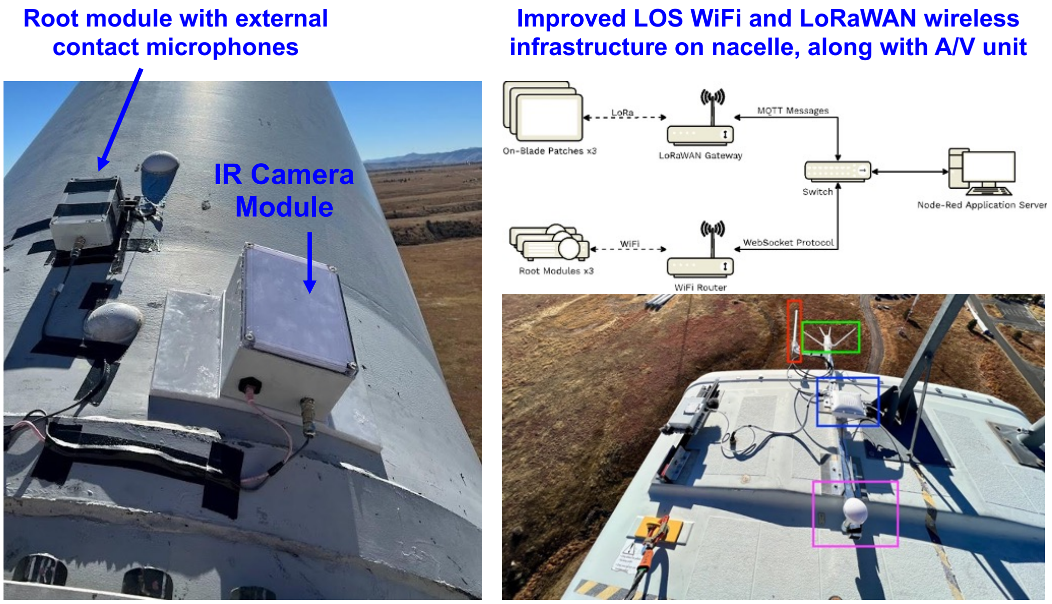
Root module with external contact microphones

Improved LOS WiFi and LoRaWAN wireless infrastructure on nacelle, along with A/V unit

Figure 16. (left) Root module sensor and IR camera module on curved mounting plate, installed near the root of a blade on a 1.5MW GE wind turbine; root modules installed on all 3 blades. (right) Improved long-range wireless (WiFi and LoRaWAN) along with A/V recording module installed on the top of the nacelle.

The above revisions and additional improvements to wireless network infrastructure and control software were implemented between the first field test (June 2021) and the second, final field test (October 2021). As before, collaborative test planning was conducted through regular meetings with NREL-NWTC staff.

4.2. Field Testing at NREL-NWTC, Boulder, CO – October 2021

Field Test Overview

Following revisions to all hardware and software systems, the complete collision detection and imaging system was again tested on an operational 1.5MW GE wind turbine at NREL-NWTC. This second up-turbine test was completed at the NREL Flatirons Campus over a period of two weeks, October 13-27, 2021. Installation of root modules, nacelle module, and all networking hardware was completed in conjunction with NREL staff using planned installation procedures and validated post-installation. The high-performance IR camera module was installed on a blade root, near one of the root module sensor enclosures. An overview of the installed modules is shown in **Fig. 16**, where spanwise and chordwise placement is the same as described in Section 4.1.

Collision Detection Testing

For primary collision detection testing, surrogate projectiles were again used. Standard tennis balls (~57g) as well as custom balsa and gelatin projectiles (25g and 40g) manufactured on-site at NREL-NWTC (examples shown in **Fig. 14**) were fired toward the turbine blade from a compressed air launcher. The lower projectile mass was increased to 25g (from 20g in prior testing) to improve tracking and increase overall hit rate percentage. Approximately 275 projectiles were launched during testing days, weather and wind allowing, with approximately 75 of these projectiles striking the blade. Testing was not conducting in the presence of lightning or nearby thunderstorms. Additionally for these tests, the blades were spinning under generation, resulting in a lower hit rate but more accurate operating conditions for the tests, but necessitating sufficient wind speeds for generation. Under these conditions, the blades rotate at approximately fixed RPM, with blade-pitch adjustments happening in real time to best mimic operational use of the systems.

Example sensor recordings are shown in the following figures (**Figs. 17-21**) for each projectile type hitting the nearer 50% blade span: tennis ball, 25g gelatin/balsa projectile, and 40g gelatin/balsa projectile.

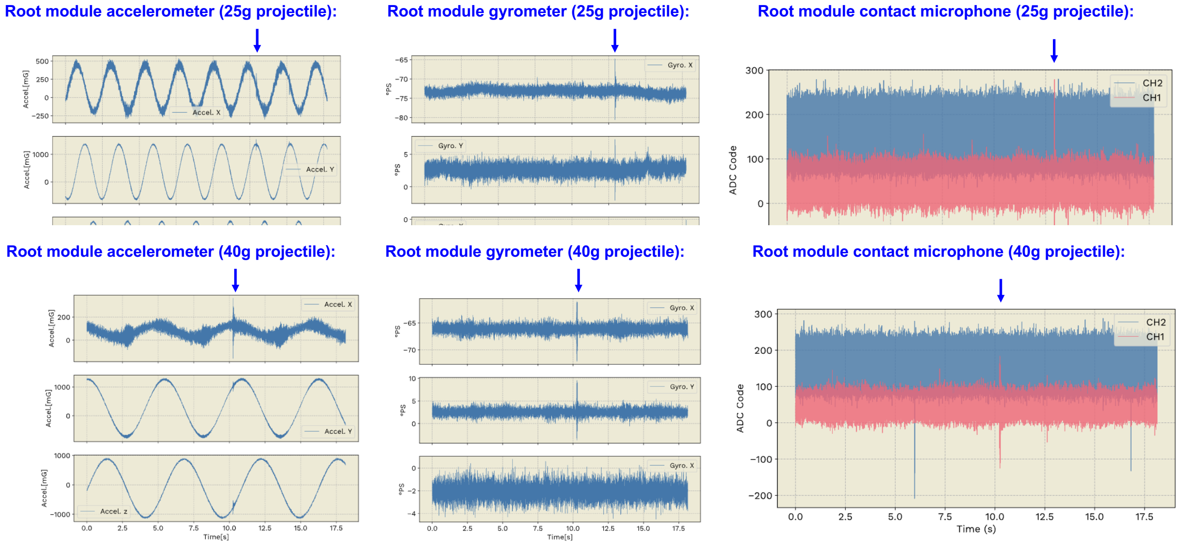

Figure 18. Typical sensor recordings for root module sensors in response to surrogate blade strike using 40g gelatin and balsa projectile: (left) 3-axis accelerometer, (middle) 3-axis gyrometer, and (right) 2-channel contact microphone. Blade strike is annotated at ~10s into the recording.

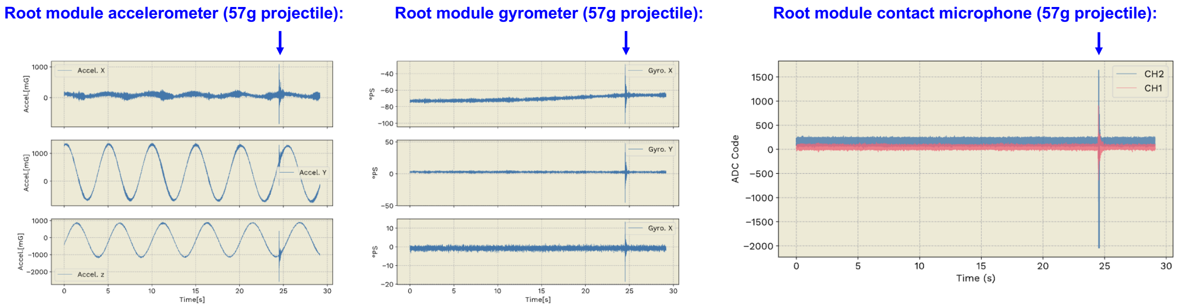

Figure 19. Typical sensor recordings for root module sensors in response to surrogate blade strike using 57g tennis ball projectile: (left) 3-axis accelerometer, (middle) 3-axis gyrometer, and (right) 2-channel contact microphone. Blade strike is annotated at ~25s into the recording.

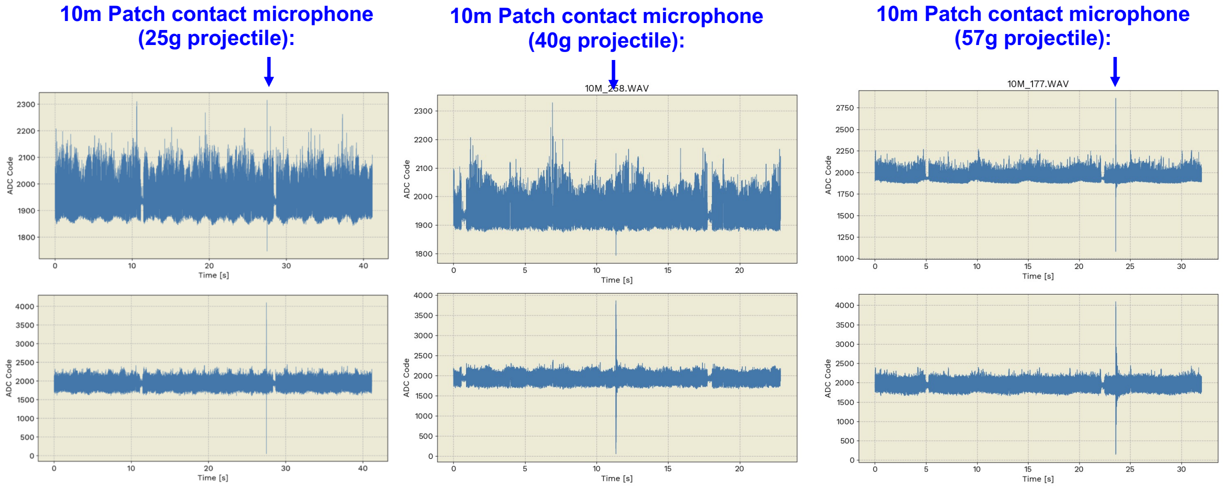

Figure 20. Typical sensor recordings for sensor patch contact microphones for patch located 10m from blade root. Each patch include two contact microphones (top, bottom of each figure) mounted orthogonally; in many cases, this results in only one microphone having a strong signal compared to baseline noise, but provides overall better coverage of possible propagating vibration signals in the blade surface for a piezoelectric contact microphone.

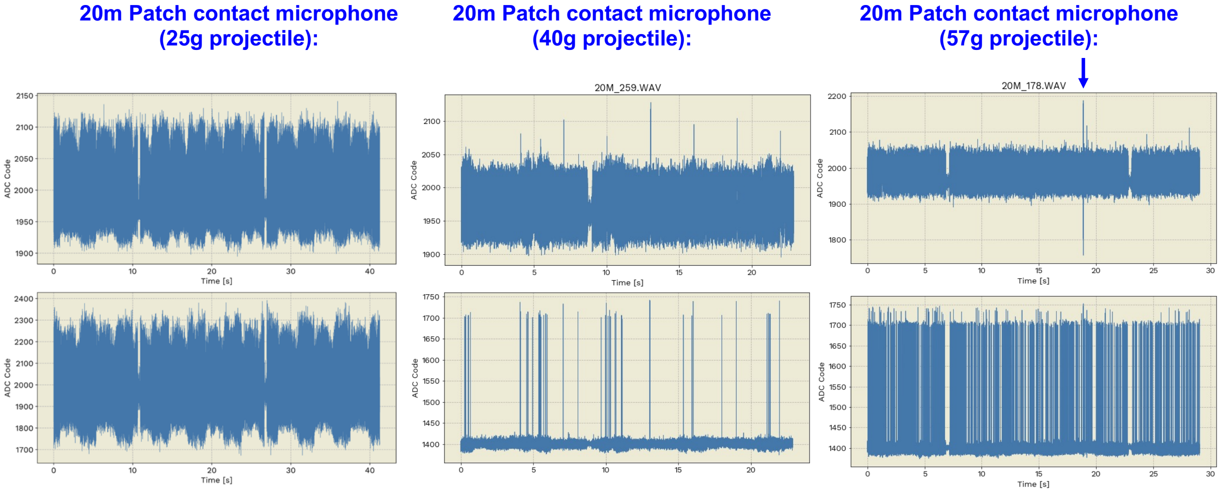

Figure 21. Sensor recordings for sensor patch contact microphones for patch located 20m from blade root. For the 25g and 40g impacts shown, the impact is not clearly visible; this is typical for an impact closer to the blade root or 10m patch. The 57g impact is still clearly visible.

Comparison of Sensor Types and Signal-to-Noise Ratio:

Analysis of a representative subset of known recorded projectile collisions from the 40g projectile data set was used to compare signal-to-noise ratio (SNR) among root module and sensor patch sensor types: accelerometer, gyrometer, and contact microphone from root module, as wells as contact microphone from 10m patch. The 20m patch data was not used, as there were not sufficient recorded collisions for a useful comparison. Examples were chosen from impacts across the blade span; close to the root is 0% span, mid-blade is 50% span, and close to the blade tip is 100% span. A summary of this analysis is shown in **Fig. 22**.

There are a few takeaways from this preliminary SNR analysis: First, the accelerometer sensor SNR is consistently higher than for gyrometer or contact microphone data. For the contact microphone, this is attributed to the mounting mechanisms. For the sensor patches, the contact microphones are internal to the self-contained module for ease of installation and are not mounted directly on the blade surface. As such, there is likely significant vibration signal loss through the adhesive, mounting plate, and base plate combined layers.

For future work, an accelerometer may be better suited to this installation method. Second, to 10m patch data has high SNR for projectiles that strike near the patch (close to 25% span for the 10m patch), and the SNR falls off with distance from the patch (further along the span). This indicates that the patch may be beneficial for collision localization, and that additional distributed patches along the blade length will provide locally enhanced SNR.

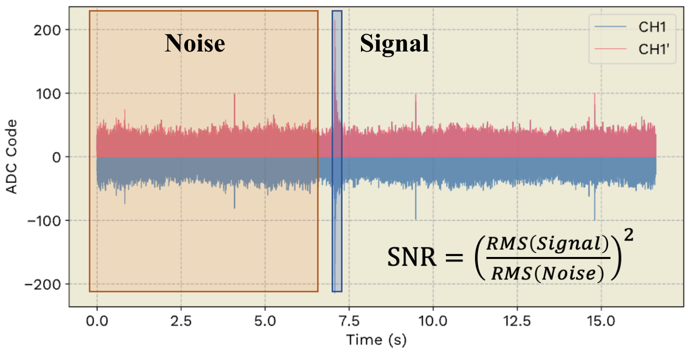

Average Blade Span	SNR Root Module Accelerometer	SNR Root Module Gyrometer	SNR Root Module Contact Mic	10m Patch Contact Mic
27 %	62.7	0	9.7	64
34 %	90	37.5	13.2	30.3
40 %	55.6	33	10.7	15.7
65 %	79.6	29	6.6	9.9

Figure 22. Example sensor recordings from the root module sensor platform, including 3-axis accelerometer and 2-channel contact microphones during a blade strike from a surrogate projectile.

Automated collision classification:

The 10m sensor patch contact microphone data recorded from the 40g gelatin and balsa wood projectile impact experiments was also used in conjunction with our previously developed collision detection algorithm [6-8] to assess automated classification performance.

The experimental data includes 23 collisions in 57 total recordings, which was labeled by hand with collisions. Data set was randomaly split into 75% and 25% portions for training and testing, respectively, using a two-step anomaly detection AdaBoost approach [8, 9-13] via SciKit-Learn [14].

An example recording is shown in **Fig. 23** (top), which highlights automatically detected anomalous frames, along with the annotated collision label. A precision-recall curve is shown in **Fig. 23** (bottom), along with true positive vs. false positive performance for the algorithm. Initial results are promising for automated classification using sensor patches and will only be improved by the inclusion of root module accelerometer signals, which have higher SNR (Fig. 22).

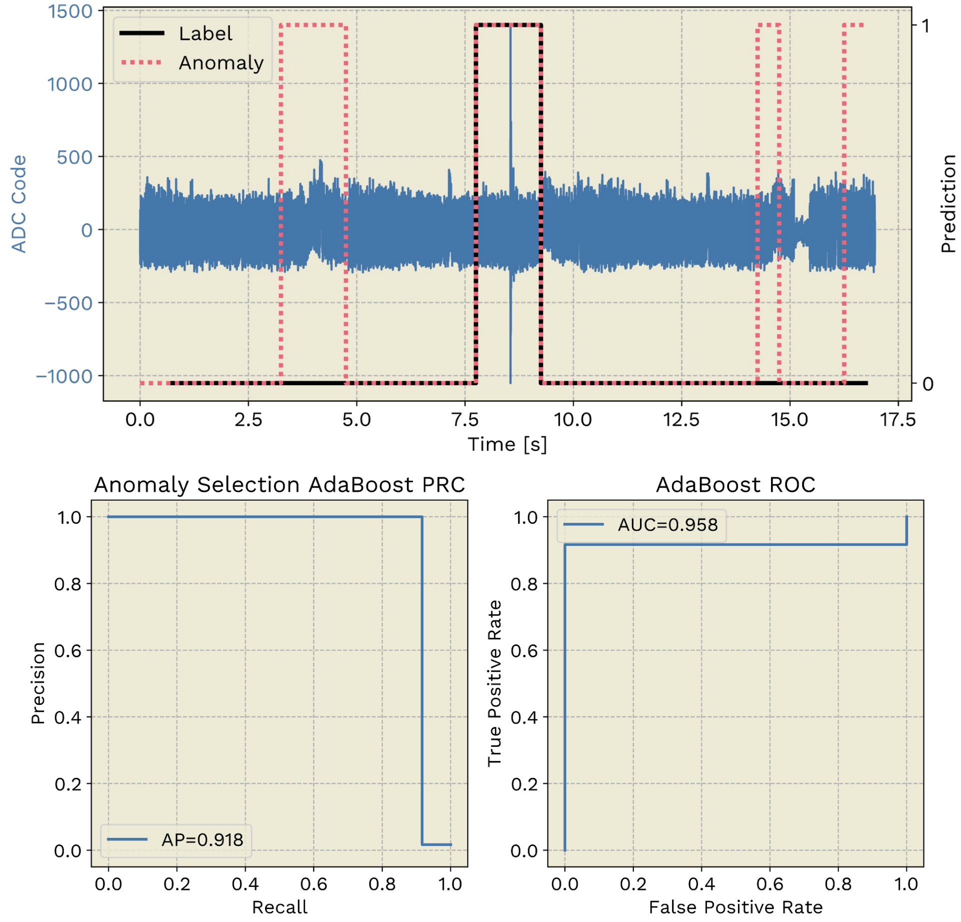

Figure 23. Example output from automated collision detection software using two-step classification [18]. Anomalous frames are identified in the first step, and among these frames containing collisions are detected using a trained AdaBoost classifier. The 'Label' indicates a labeled collision (e.g. ground truth) in the hand-annotated training/testing data set, for which collisions are known from field test notes.

High-performance IR camera recordings from on-blade module:
The high-performance IR camera module was tested using heated and cooled projectiles for assessing the application of this imaging technology to extend system performance, especially for nighttime use. During field testing, which was limited to daytime operations, cooled projectiles provided a higher contrast to background and were primarily using for imaging and tracking tests. Shown in **Fig. 24** is a frame from a video recording taken from the blade-mounted IR camera module (**Fig. 16**) in which a cooled projectile (tennis ball) is seen just prior to collision with the wind turbine blade (left); color inversion emulates what a heated object would appear in dark background (right).

We applied an automated object detection and tracking technique, YOLOv4 [15,16], for automated detection of the tennis ball, with example results shown in **Fig. 25**. For a static blade, the projectile is detected with high confidence (left), however detection fails during blade rotation (right), attributed primarily to background blur. Images are recorded at 640x480 resolution at 30 frames per second (fps).

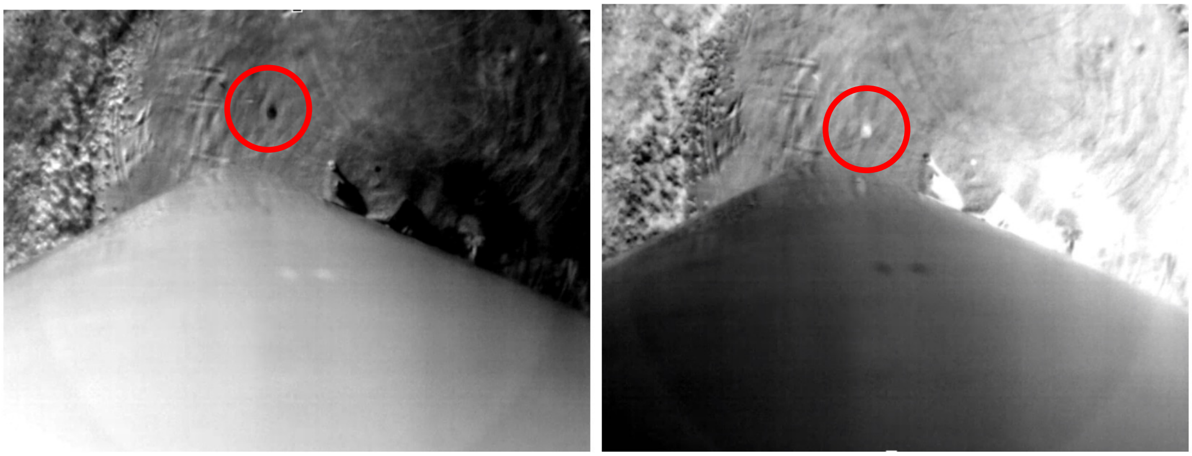

Figure 24. Images recorded using the high-performance IR camera (Sierra Olympic Vinden 75LR) mounted near the blade root in a custom enclosure. (left) IR image showing blade surface and cool (black) tennis ball projectile, manually annotated by a red circle. (right) The same recorded image with color inversion, showing projectile as a hot (white) object, manually annotated by a red circle.

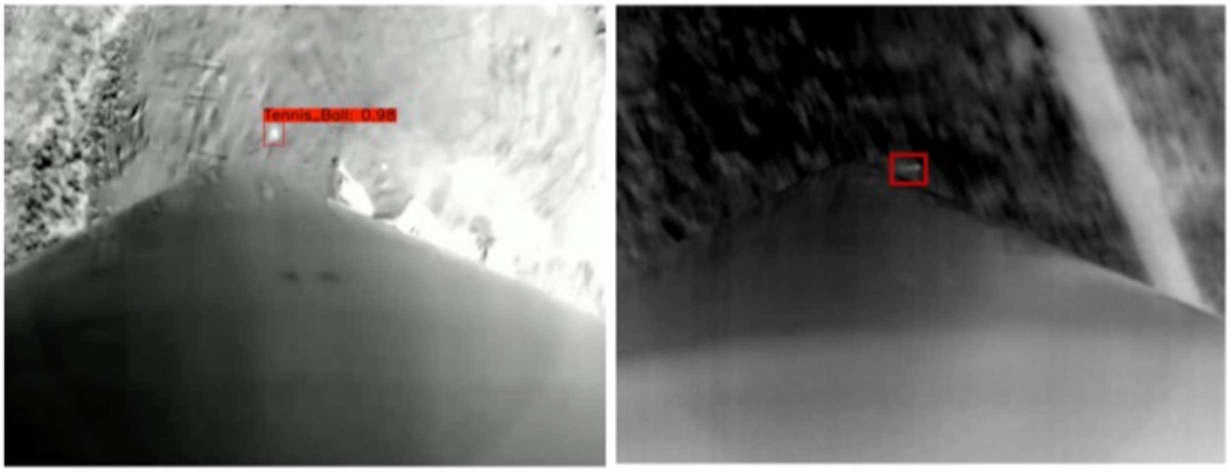

Figure 25. (left) Tennis ball is automatically detected and tracked across frames, enabling trajectory estimation; blade is not rotating. (right) Background blur in rotating blade camera recording prevents automated detection and tracking of the projectile using current approaches.

5. Conclusions and Suggested Future Work

5.1. Overall system validation:

Final field testing at NREL-NWTC demonstrated successful operation of the complete collision detection system, including blade root modules and distributed sensor patches, for continuously collecting a combination of contact microphone and accelerometer data from the blade surface during surrogate collisions, and providing both local data storage and wireless system communication and control. Installed down-blade sensor patches operated continuously for more than two weeks without battery recharging, and all indications point to their being sufficiently low power to operate indefinitely from the integrated photovoltaic energy harvesters. Both low-cost imagers integrated into the root module and high-performance IR camera returned useful images, and analysis of these is ongoing for automated object tracking. Overall, approximately 275 projectiles yielded 75 surrogate collisions, and initial testing of the new data set with our previously developed collision detection algorithm show significant promise for automated collision detection (Average precision = 0.918) and image capture for wind turbine blade strikes.

Standalone characterization of the collision detection system using a wind turbine blade on the ground demonstrated even higher sensitivity and limits of detection for objects as small as 2.5g at ~10 m/s. While this is without the presence of background noise expected up-turbine, it demonstrates promise for further improvements in collision detection performance as algorithm development progresses.

The data sets collected across two up-turbine field tests include multi-channel accelerometer and contact microphone data recorded from three sensor root modules, three down-blade sensor patches across more than a hundred surrogate blade strikes, as well two CMOS imagers on each of three wind turbine blades and the single high-performance IR camera module, provide a rich data set for continued development and testing of collision detection algorithms and image processing approaches. Analysis is ongoing, and promising results will be disseminated in future publications as appropriate.

5.2. Long-term considerations:

A number of issues were raised during the development, validation, and deployed testing of the integrated collision detection and imaging system, both through our own work and through multiple conversations with wind turbine operators, engineers, wildlife biologists, and other stakeholders; we summarize some of the high-level considerations here to inform future development for collision detection systems:

False Detections: All detection systems of nontrivial sensitivity will produce false positive classifications given enough operating time. For blade strike detection, this may include collisions detected from precipitation (e.g. rain, snow, or hail), high wind conditions, or other weather-related events that impart sudden vibrations to the blade but are not due to wildlife interactions. These would need to be separated from wildlife-related blade strikes using the collected images, either offline by trained personnel or in real-time using trained classification algorithms.

Long-term Maintenance: In offshore environments, salt spray will collect on image surfaces and degrade image quality over time; the corresponding maintenance timelines were not assessed in this project but would be an important consideration for future development. The core vibration-based collision detection systems are less impacted by these affects, although photovoltaic energy harvesting will similarly degrade over time due to occlusions and require maintenance.

Aerodynamic Effects: Sensors installed externally on the wind turbine blade surface will have an effect on blade aerodynamics and generation efficiency. This can be mitigated but not eliminated by low profile form factors and proper cord-wise placement, and as such would be an important consideration for long-term deployed use. We note that the collision detection system is expected to work as well or better if installed internally to the blade during manufacture, removing the aerodynamic implications. While cameras would still need to be external for image capture, these are located near the hub (or on the tower or nacelle) and have much less aerodynamic effect.

6. Acknowledgments

We are greatly indebted to our collaborators at the National Renewable Energy Laboratory National Wind Technology Center at the NREL Flatirons Campus, with special thanks to Samantha Rooney, Jason Roadman, and Chris Ivanov. We thank Department of Energy program managers and grant administrators for their guidance and support of this project.

7. References

1. T.D. Allison, J.E. Diffendorfer, E.F. Baerwald, J.A. Beston, D. Drake, A. M. Hale, C. D. Hein, M. M. Huso, S. R. Loss, J. E. Lovich *et al.*, "Impacts to wildlife of wind energy siting and operation in the United States," *Issues in Ecology*, vol. 21, pp. 1–24, 2019.
2. E.B. Arnett and R.F. May,"Mitigatingwindenergyimpactsonwildlife: approaches for multiple taxa," *Human–Wildlife Interactions*, vol. 10, no. 1, p. 5, 2016.
3. R. May, A. B. Gill, J. Ko¨ppel, R. H. Langston, M. Reichenbach, M. Scheidat, S. Smallwood, C. C. Voigt, O. Hu¨ppop, and M. Portman, "Future research directions to reconcile wind turbine–wildlife interactions," in *Wind Energy and Wildlife Interactions*. Springer, 2017, pp. 255–276.
4. K. C. Sinclair, "Approaches to addressing environmental challenges with wind energy in the United States," National Renewable Energy Lab. (NREL), Golden, CO (United States), Tech. Rep., 2017.
5. "Bird Impact Forces and Pressures on Rigid and Compliant Targets", Technical Report, U.S. Air Force Flight Dynamics Laboratory, AFFDL-TR-77-60, May 1978.
6. Clocker, K., Hu, C., Albertani, R., and M.L. Johnston, "Sensor System and Signal Processing for Automated Blade Collision Detection on Wind Turbines", *IEEE SENSORS 2020*, Rotterdam, Netherlands (Virtual), pp. 1-4, Oct. 2020.
7. C. Hu and R. Albertani, "Machine learning applied to wind turbine blades impact detection," *Wind Engineering*, p. 0309524X19849859, 2019.
8. K. Clocker, C. Hu, R. Albertani, and M.L. Johnston, "Autonomous sensor system for wind turbine blade collision detection," *IEEE Sensors Journal*, vol. 22, no. 12, pp. 11382-11392, 2022.
9. Y. Freund and R. E. Schapire, "A decision-theoretic generalization of on-line learning and an application to boosting," in European conference on computational learning theory. *Springer,* 1995, pp. 23-37.
10. L. Breiman, "Random forests," *Machine learning*, vol. 45, no. 1, pp. 5-32, 2001.
11. Y. Freund, R. Schapire, and N. Abe, "A short introduction to boosting," *Journal-Japanese Society for Artificial Intelligence,* vol. 14, no. 771- 780, p. 1612, 1999.
12. J. Solimine, C. Niezrecki, and M. Inalpolat, "An experimental investigation into passive acoustic damage detection for structural health monitoring of wind turbine blades," *Structural Health Monitoring,* vol. 0, no. 0, p. 1475921719895588, 0.
13. T. Hastie, S. Rosset, J. Zhu, and H. Zou, "Multi-class AdaBoost*," Statistics and its Interface*, vol. 2, no. 3, pp. 349-360, 2009.
14. F. Pedregosa, G. Varoquaux, A. Gramfort, V. Michel, B. Thirion, O. Grisel, M. Blondel, P. Prettenhofer, R. Weiss, V. Dubourg, J. Vander- plas, A. Passos, D. Cournapeau, M. Brucher, M. Perrot, and E. Duch- esnay, "Scikit-learn: Machine learning in Python," *Journal of Machine Learning Research,* vol. 12, pp. 2825-2830, 2011.

15. Pierrick Rugery. Explaining yolov4 a one stage detector. Technical Paper: Becoming Human: Artificial Intelligence Magazine, Sep 2020.
16. Xu Zhang, Xiangyang Hao, Songlin Liu, Junqiang Wang, Jiwei Xu, and Jun Hu. Multi-target tracking of surveillance video with differential YOLO and DeepSort. In Jenq-Neng Hwang and Xudong Jiang, editors, Eleventh Interna- tional Conference on Digital Image Processing (ICDIP 2019), volume 11179, pages 701 - 710. International Society for Optics and Photonics, SPIE, 2019.
17. Albertani, R.; Clocker, K.; Hu, C.; Johnston, M. (2021). *Final Technical Report: A Heterogeneous System for Eagle Detection, Deterrent, and Wildlife Collision Detection for Wind Turbines*. Report by Oregon State University. Report for US Department of Energy (DOE). Report for Office of Energy Efficiency and Renewable Energy (EERE).
18. K. Clocker, C. Hu, R. Albertani, and M.L. Johnston, "Autonomous sensor system for wind turbine blade collision detection," *IEEE Sensors Journal*, vol. 22, no. 12, pp. 11382-11392, 2022.